A Compact 5GHz Q-enhanced Standing-Wave Resonator-based Filter in 0.13μm CMOS

Dan Shi and Michael P. Flynn

University of Michigan, Ann Arbor, MI, 48109

***Abstract* — A fully-integrated 5GHz bandpass filter with 0dB IL and 3dB bandwidth of 9.5% (1dB bandwidth of 6%) is reported. The filter employs novel on-chip capacitively-loaded, transmission-line standing-wave resonators and Q-enhancement circuits. A prototype 5GHz on-chip filter, implemented in 0.13μm CMOS, dissipates 2.88mW from a 1.2V supply, and occupies a die area of 0.3mm^2.**

Index Terms* — *filter, Q-enhanced, CMOS, transmission line, resonator.

I. Introduction

The insertion loss and the bandwidth of integrated on-chip filter are limited by the low quality factor of on-chip inductors. At 5GHz, inductor Q typically ranges from 5 to 15. To overcome this problem, Q-enhanced LC bandpass filters have been studied [1-3]. A critical problem faced with this type of on-chip filter is the high power consumption required to achieve low insertion loss and acceptable dynamic range. At higher frequencies this problem gets worse since inductor Q typically is smaller.

Capacitive termination in the resonators reduces the required length of the transmission line; while periodic capacitive-loading reduces wave-velocity and wavelength to a fraction of the already reduced value. Similar techniques are employed for VCO design in a compact 5GHz standing-wave resonator-based VCO reported [4]. A higher Q is achieved since a short transmission line has low substrate and Ohmic losses. Finally, the insertion loss is further reduced with a simple Q-enhancement scheme.

II. Filter Design

As shown in Figure 1(a), the prototype direct-coupled 2-pole filter consists of two resonators, a negative transoductance (g_m) and matching circuits. A coupled resonator structure similar to that proposed and implemented on a Duroid substrate in [5] is adopted. To make this resonator structure practical for on-chip implementation, techniques are introduced to improve and enhance-Q. Standing-wave resonators (with simulated Q of 35) are used to reduce the insertion loss and power consumption. Negative g_m circuits are utilized to overcome loss in the resonators, so that the insertion loss is further reduced. Matching circuits are used to form 50 Ohms input and output impedances.

The equivalent circuit of the coupled resonators is shown in Figure 1(b), where the series L-C on the left and right is equivalent circuit of a Q-enhanced resonator. Coupling between resonators is predominantly magnetic, since at resonance the electrical field in the resonators is maximized near the open-gap side while the magnetic field is maximized at the opposite side [5]. This magnetic dominant coupling can be modeled as an inductor-formed impedance inverter in Figure 1(b).

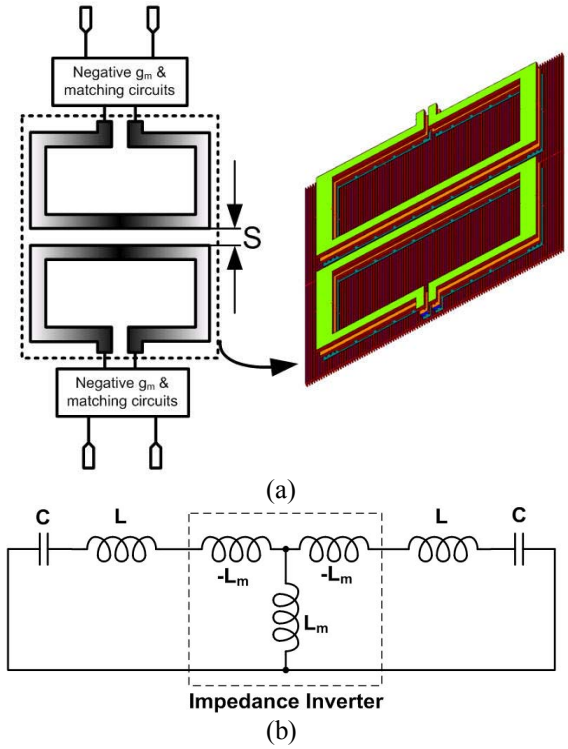

Figure 1: (a). Block diagram of the direct coupled 2-pole filter. (b). Equivalent circuit of coupled resonators.

Figure 2(a) shows the side view of the resonator which consists of a thick metal rectangular open loop over a thin floating metal shield. To reduce Ohmic losses, the metal conductor of the resonator is formed with the top three metal layers, shorted together with vias. A floating metal shield is formed with floating metal strips, with each strip formed with strips in each of the lower five metal layers connected in parallel. The strip structure breaks induced Eddy currents. When the resonator is differentially connected, the floating metal shield is a virtual ground, which provides a better shield to the lossy substrate. The top of the floating metal shield is relatively close to the

conductor (only 1.4μm away), so that the shield deliberately loads the resonator with capacitances. The transmission line with a close by metal shield can be modeled as an LC ladder (Figure 2(b), where L is series inductance per unit length and C is shunt capacitance per unit length). Capacitors C_p model the capacitor between transmission line and shielding layers. The new equivalent capacitance is $C+C_p$ and the phase velocity is:

$$v_p = \frac{1}{\sqrt{(C + C_p)L}}, \quad (1)$$

which is smaller than without metal shielding. This introduces the slow-wave effect [6]. (H.M. Barlow [7] first demonstrated the slow wave effect by placing an array of uniformly spaced parallel wires along a rectangular waveguide.) Since wave-velocity and wavelength are reduced, the slow wave effect allows size to be reduced, and the quality factor to be increased.

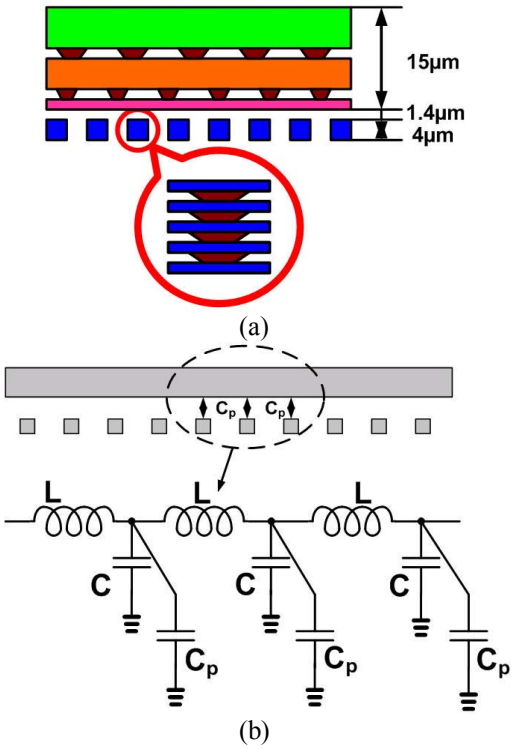

Figure 2: (a) Capacitively-loaded slow-wave transmission line resonator; (b) Transmission line with metal shields and the corresponding equivalent circuit.

In this work, the length of the transmission line is shortened to below a half wavelength at resonant frequency by terminating the differential transmission line with capacitors. Normally the length of a resonator transmission lines at resonance is $\lambda_0/2$. However as predicted in [8], shorter transmission lines have a larger Q at resonant frequency. A shorter transmission line can be used to achieve the same resonance frequency if the ends of the shorter transmission line are terminated with capacitance [9]. Figure 3 shows the equivalence between capacitor loaded transmission line resonator and unloaded transmission line resonator. The relationship between loading capacitor and reduced transmission line length is determine by

$$C = \frac{\tan\theta_2}{Z\omega}, \quad (2)$$

where θ_2 is the effective reduction in electrical length (a multiple or submultiple of the wavelength), ω is the resonant frequency, and Z is the impedance [8].

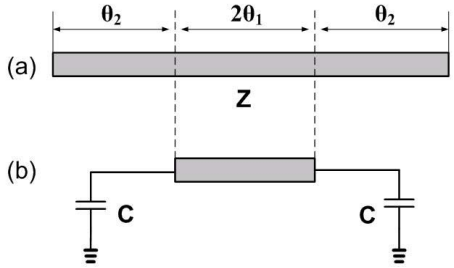

Figure 3: (a) Unloaded transmission line resonator. (b) Loaded transmission line resonator.

To achieve an optimum Q for a given resonance frequency, the tradeoff between line length and capacitance is optimized following the methods described in [4]. In the final design, capacitors of 3pF are loaded at the two ends of the resonator transmission line. The combination of the slow-wave-effect and capacitive loading at the ends reduces the length of the transmission line to only $0.04\lambda_0$ (λ_0 is the wavelength in free space).

The coupling coefficient between the two resonators is determined using the pole splitting method [5] in conjunction with a 3D EM simulator (Zeland IE3D). In the pole splitting method, the relationship between the frequency separation of the poles and the coupling coefficient is determined by:

$$K = \frac{f_a^2 - f_b^2}{f_a^2 + f_b^2} = \frac{L_m}{L}, \quad (3)$$

where f_a and f_b are the frequencies of the two poles, L_m and L are the inductance values in the equivalent circuit shown in Figure 1(b). Figure 4 shows the coupling coefficient (K) as a function of the horizontal distance between two resonators. Based on these values a 2-pole Chebyshev bandpass filter is designed. The simulated

filter center frequency is 5.2GHz and the bandwidth is 8%.

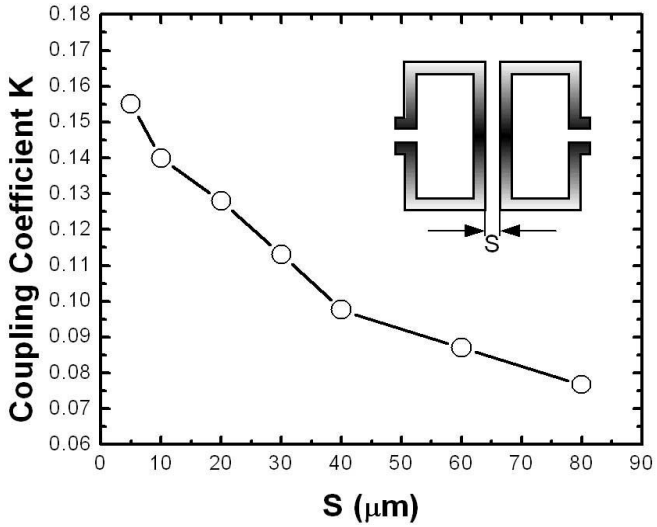

Figure 4: Simulated coupling coefficients as a function of the horizontal separation between the resonators

III. Q-Enhanced Circuit and Impedance Match

Figure 5a shows schematics of the negative g_m circuit and matching circuit blocks in the filter block diagram. The cross-coupled FETs introduce negative resistance. Current reuse due to the use of NMOS and PMOS cross coupled FETs improves power efficiency. Two sets of capacitors (C1-C4) with a impedance transformation ratio of 4impedance match resonator high impedance to 50 Ohms (Figure 5b). These capacitors also form loading capacitors (C_t in Figure 5b) at the ends of resonators.

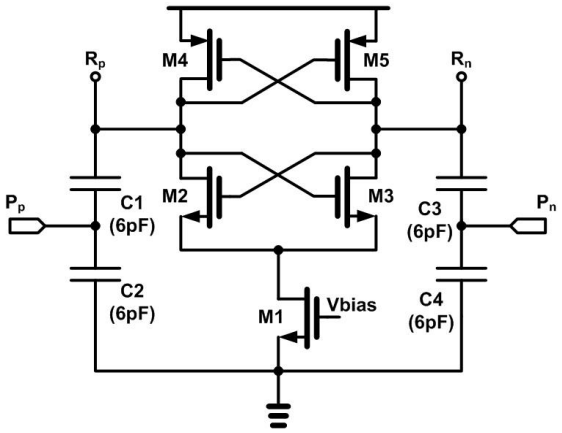

(a)

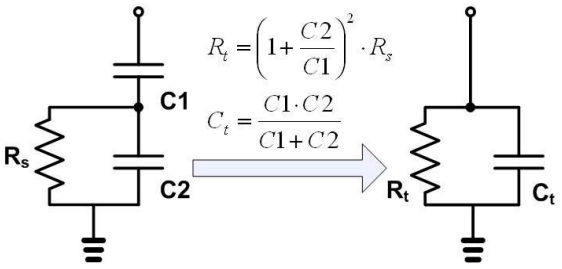

(b)

Figure 5: (a) Q-enhacement and matching circuit schematic (R_p and R_n are connected the resonator). (b) impedance transformation.

IV. Measurement Results

The prototype is fabricated in an 8-level-metal 0.13μm CMOS process with a 4μm thick top aluminum layer. A die micrograph is shown in Figure 6. The filter occupies 0.3mm^2 and the total die area including pads is 0.6mm^2. The filter transfer S_{21} characteristic, measured with GSSG probes, is shown in Figure 7. An insertion loss of 0dB is achieved at 5.03GHz with 9.7% 3dB bandwidth. To measure the in-band IIP3, two signals close in frequency (one at 5GHz and the other at 5.1GHz) at different power levels were introduced into the filter. Care was taken to ensure the third-order IM lies well within the filter passband. For the out-of-band case, two out-of-band signals (one at 5.6GHz and the other at 6.2GHz) at different levels were introduced into the filter, again keeping the third-order IM well within the filter passband. Figure 8 shows the measured IIP3, where the in-band and out-of-band IIP3 are -8.0dBm and 7.8dBm, respectively.

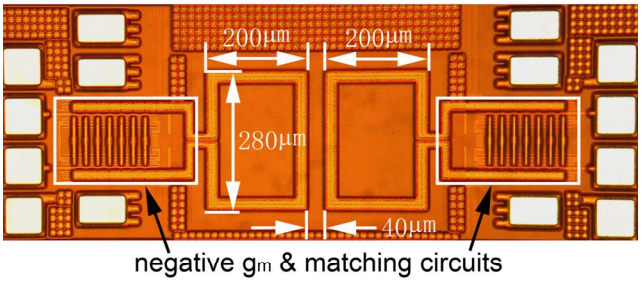

Figure 6: Die micrograph.

The filter core draws 2.4mA from a 1.2V supply. Table I summarize the measured performance of the on-chip filter. This prototype is compared with other recently published Q-enhanced filters. This prototype on-chip resonator based filter outperforms most recently published CMOS on-chip filter in terms of power consumption and die area.

TABLE II: COMPARISON.

Reference	Technology	f_0 (GHz)	Gain (dB)	Power Supply (V)	P_{DC} (mW)	BW	Die area (mm^2)	P_{1dB} (dBm)	Dynamic Range (dB)
This work	CMOS 0.13µm	5.03	0	1.2	2.88	9.5% (6% -1dB BW)	0.3	-16.7	77.3
[1]	CMOS 0.35µm	2.19	-10-0	1.3	5.0	2.4%	0.1	-30	38
[2]	CMOS 0.25µm	2.14	0	2.5	17.5	2.8%	3.5	-13.4	56
[3]	CMOS 0.8µm	0.84	0	2.7-3.0	77	2.1%	2	-18	75

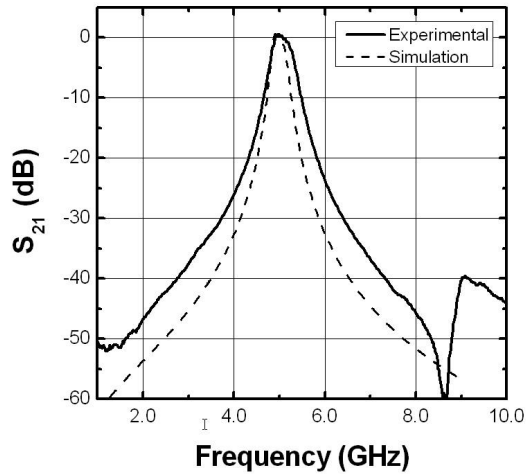

Figure 7: Measured and simulated filter transfer response.

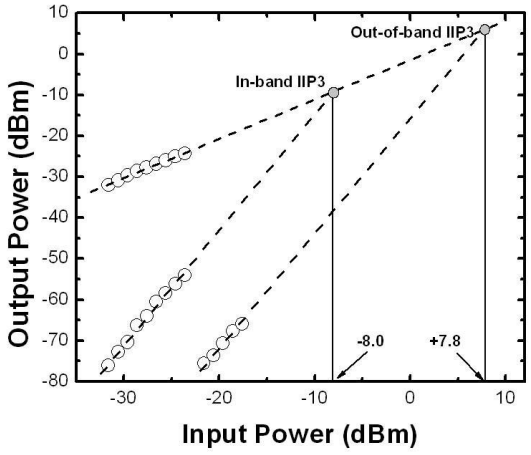

In-band IIP3 out-of-band IIP3

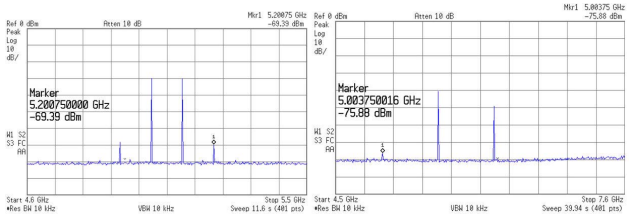

Figure 8: Measured in-band, out-of-band IIP3, and corresponding output spectrums.

Table I: Measured filter performance summary.

Center Frequency	5.03GHz
Bandwidth	9.5% (-3dB), 6% (-1dB)
Input 1dB Compression	-16.7dBm
Output Noise Floor	-94dBm
In-band dynamic range	77.3dB
In-band IIP3	-8.0dBm
Out-of-band IIP3	7.8dBm
Supply Voltage	1.2 V
Power Consumption	2.88mW
Die Area	$0.3mm^2$

ACKNOWLEDGEMENTS

The authors acknowledge the assistance of Zeland and MOSIS. This work was supported by the WIMS-ERC, Engineering Research Centers program of the NSF under Award Number EEC-9986866.

REFERENCES

[1] F. Dulger, E. Sanchez-Sinencio, and J. Silva-Martinez, "A 1.3-V 5-mW fully integrated tunable bandpass filter at 2.1 GHz in 0.35µm CMOS," *IEEE J. Solid State Circuits,* vol. 38, pp. 918-928, 2003.

[2] T. Soorapanth and S. S. Wong, "A 0-dB IL 2140±30 MHz bandpass filter utilizing Q-enhanced spiral inductors in standard CMOS," *IEEE J. Solid State Circuits,* vol. 37, pp. 579-586, 2002.

[3] W. B. Kuhn, N. K. Yanduru, and A. S. Wyszynski, "A high dynamic range, digitally tuned, Q-enhanced LC bandpass filter for cellular/PCS receivers," *IEEE MTT-S Symp. Dig.*, 1998, pp. 93-97 vol.1.

[4] D. Shi, J. East, and M. P. Flynn, "A Compact 5GHz Standing-Wave Resonator-based VCO in 0.13µm CMOS," *IEEE RFIC Symp. Dig.*, 2007, pp. 591-594.

[5] H. Jia-Sheng and M. J. Lancaster, "Couplings of microstrip square open-loop resonators for cross-coupled planar microwave filters," *IEEE Trans. Microw. Theory Tech.,* vol. 44, pp. 2099-2109, 1996.

[6] T. S. D. Cheung, J. R. Long, K. Vaed, R. Volant, A. Chinthakindi, C. M. Schnabel, J. Florkey, and K. Stein, "On-chip interconnect for mm-wave applications using an all-copper technology and wavelength reduction," *ISSCC Dig. Tech. Papers*, 2003, pp. 396-501 vol.1.

[7] H. M. Barlow, "Dipole-type-mode propagation in a rectangular waveguide," *Proc. IEE,* vol. 121, pp. 1363-1366, 1974.

[8] D. M. Pozar, *Microwave engineering*, 2nd ed. New York: Wiley, 1997.

[9] H. Jia-Sheng and M. J. Lancaster, "Theory and experiment of novel microstrip slow-wave open-loop resonator filters," *IEEE Trans. Microw. Theory Tech.,* vol. 45, pp. 2358-2365, 1997.